Determining the temporally and radially resolved temperature distribution inside a pulsed broad-area vertical-cavity surface-emitting laser cavity

Shyam K. Mandre and Wolfgang Elsäßer
Institute of Applied Physics, Darmstadt University of Technology, Schlossgartenstrasse 7, D-64289 Darmstadt, Germany

Ingo Fischer,[a] Michael Peeters, and Guy Verschaffelt
Department of Applied Physics and Photonics, Vrije Universiteit Brussel, Pleinlaan 2, B-1050 Brussels, Belgium

(Received 14 June 2006; accepted 24 August 2006; published online 9 October 2006)

The authors experimentally determine temporally and radially resolved profiles of the temperature distribution within the cavity of a broad-area vertical-cavity surface-emitting laser in pulsed operation. For this, the recently discovered state of spatially incoherent emission [M. Peeters *et al.*, Opt. Express **13**, 9337 (2005)] is harnessed. Using single-shot measurements of spectrally resolved near field profiles acquired by a fast-gated charge coupled device camera, the wavelength shift due to heating of the device is temporally and radially resolved. From the wavelength shift the temperature shift is extracted, which finally allows for determination of absolute temperature profiles. © *2006 American Institute of Physics*. [DOI: 10.1063/1.2361164]

Motivated by the successful commercial deployment of vertical-cavity surface-emitting lasers (VCSELs) in recent years, the development of high-power VCSELs has gained significant interest. In particular, the possibility to integrate large numbers of VCSELs into two-dimensional arrays promises optical output powers of several watts.[1] Broad-area (BA-) VCSELs with aperture diameters up to typically 100 μm have been realized, which can achieve cw output powers of up to ~100 mW from a single device. A limitation to the attainable output powers is imposed by Joule heating due to the high current densities.[1] From a technological point of view, detailed insight into the heat management and transport within the devices can allow optimization of the VCSELs' thermal properties and, subsequently, enhancement of their optical performance.[2–5] Techniques based on Raman scattering (micro-Raman),[6] spontaneous electroluminescence,[7] or temperature-dependent reflectance[8] have been presented, with which the temperature in edge-emitting semiconductor lasers and in VCSELs was determined, respectively. Complementary to these techniques, we present an alternative method to experimentally determine *temporally resolved* radial profiles of the temperature distribution within the aperture of a BA-VCSEL, harnessing the recently published spatially incoherent state of emission of the BA-VCSEL in pulsed operation.[9]

The experimental setup is schematically depicted in Fig. 1. The emission of the 50 μm diameter BA-VCSEL's facet which we refer to as near field (NF) is imaged onto the input slit of a 1 m Czerny-Turner imaging spectrometer. The spectrally dispersed NF profile is then imaged onto a fast-gated intensified charge coupled device camera (4picos, Stanford Computer Optics, Inc.) with exposure times of 300 ps. With this camera, it is possible to study the emission properties of the BA-VCSELs on such short time scales. A pulse generator is used to drive the BA-VCSEL with rectangular pulses of ~30 μs width, triggered at 50 Hz by the camera. The duty cycle is kept small (<0.5%) to ensure that the VCSEL cools down to the mount temperature controlled at 28 °C between consecutive pulses. An adjustable delay line allows acquisition of single-shot events at different times during the applied pulse.

Figure 2 depicts a sequence of single-shot measurements of spectrally dispersed NF profiles at different temporal positions τ (τ: time after onset of laser emission). These optical spectra depict a radial (spatial) dimension of the BA-VCSEL's NF in the vertical direction and the spectral dispersion of the NF profile in the horizontal direction. The total spectral width shown in Fig. 2 amounts to about 18 nm. Obtaining optical spectra with this method has the advantage that spatial resolution is maintained even in the horizontal direction.[10] The sequence shows the evolution of the BA-VCSEL's spectral emission properties in pulsed operation with a current amplitude of the electrical pulses of $11I_{\mathrm{thr}}$ ($\approx$160 mA). The first spectrum ($\tau \sim 0.02$ μs) reveals emission in high-order transverse modes on the short-wavelength side of the spectrum and a cloud of modes which cannot be resolved on the long-wavelength side. During the next microsecond of the pulse, a dynamic transition of the emission takes place, leading to a curved optical spectrum ($\tau \sim 1$ μs) resembling the shape of a parabola. This transition is discussed in greater detail elsewhere.[11] The width of the parabo-

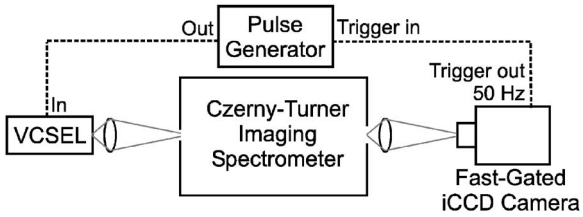

FIG. 1. Schematic of the experimental setup used to acquire single-shot measurements of the BA-VCSEL's spectrally dispersed near field profiles. The temporal resolution/exposure time is 300 ps.

[a]Electronic mail: ifischer@tona.vub.ac.be

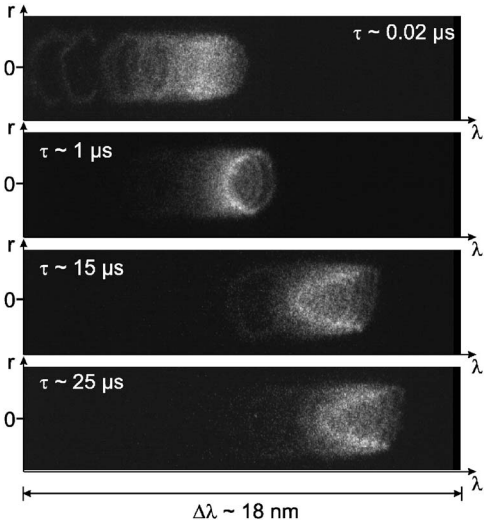

FIG. 2. Sequence of single-shot measurements of the BA-VCSEL's spectrally dispersed near field profiles at different temporal positions τ. The current amplitude of the 30 μs long electrical pulses is $11I_{\mathrm{thr}}$ ($\approx$160 mA).

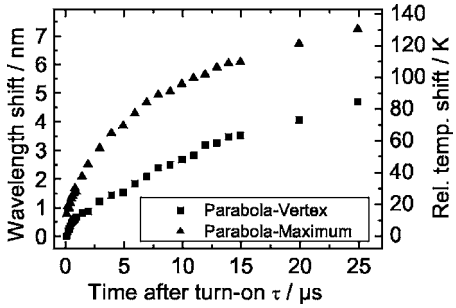

FIG. 3. Wavelength shift and relative temperature shift of the BA-VCSEL's emission. The spectral positions were obtained by determining the positions of the parabola vertices (squares) and parabola maxima (triangles) in the single-shot measurements recorded at different τ. The BA-VCSEL was operated with the same conditions as in Fig. 2.

lalike spectrum initially increases and then remains constant after $\tau \sim 7$ μs. In addition, a significant redshift of the emitted spectrum can be observed in the sequence. This wavelength shift amounts to about 6 nm within the first 30 μs of emission. Note that, e.g., at $\tau \sim 1$ μs, distinct wavelengths are emphasized, leading to pronounced curved lines. The exact origin of these lines requires further detailed studies.

We have verified that the occurrence of the parabola-shaped optical spectra is linked to emission in independent coherence islands with dimensions of a few microns.[9,11] The loss of spatial coherence is the result of the combination of a fast thermal chirp (observed as the wavelength shift) and a thermal lens, which together prevent the buildup of transverse modes. Based on the previous characterization, we interpret the wavelength of the locally emitted spatially incoherent light to be determined by the local cavity conditions, i.e., the optical resonator length L_{opt} at the position of the individual coherence islands. The dependence observed here reveals that L_{opt} is not constant across the cavity. In case of emission in transverse modes, the modes would be defined by the global cavity. The spectral positions of the modes thus would not contain information about the local cavity properties.

As is well known, the optical resonator length increases with increasing temperature. Furthermore, the emitted wavelength λ is proportional to the optical resonator length. Therefore, the emitted wavelength increases with increasing temperature. From the parabolalike spectra in Fig. 2, one can deduce that the emission wavelength in the outer regions of the BA-VCSEL's aperture is longer than that in the central region. Therefore, the temperature in the outer regions is higher than in the center. Using single-shot measurements of the spectrally dispersed NF profiles of the BA-VCSEL's (incoherent) emission, we have extracted temperature profiles by relating shifts in the locally emitted wavelength to local temperature changes.

Figure 2 reveals a wavelength shift of the BA-VCSEL's emission which can be attributed to heating of the device (thermal chirp) during the applied pulse. The wavelength shift in dependence on τ is plotted in Fig. 3 (left-hand scale), where the squares denote the spectral positions of the emission at the center of the BA-VCSEL aperture (parabola vertices) and the triangles denote the spectral positions of the emission at the outer regions of the VCSEL aperture (parabola maxima). Figure 3 shows a wavelength shift of the maxima of more than 6 nm within the first 25 μs of emission, whereas the vertex shifts only about 5 nm. The difference in the wavelength shifts can be related to radially inhomogeneous heating of the VCSEL. The temperature in the outer regions of the BA-VCSEL aperture (maximum) is higher and increases faster than in the center (vertex). Using the measured wavelength shifts, it is possible to determine relative temperature shifts. For this, we first determine the temperature-dependent wavelength shift of the BA-VCSEL given by $\Delta\lambda = a\Delta T$ (ΔT is the temperature shift and a is the temperature coefficient) by varying the heat-sink temperature and recording the emitted wavelength. From this experiment we determined a to be 0.056 nm/K which is then used to derive the relative temperature shift also depicted in Fig. 3, now using the right-hand scale. The relative temperature shift at the VCSEL's center was set to 0 K for $\tau \sim 100$ ns, the first occurrence of the parabola in the spectra. We can now determine the heating of the device relative to this starting temperature in the VCSEL's center. For example, the starting temperature of the outer rim is about 14 K higher than that in the center. The temperature in the center increases by approximately 80 K within the first 25 μs of emission, while the temperature in the outer rim increases by about 120 K during the same time. The influence of an inhomogeneous current profile on the refractive index has been neglected here. Applying previous results[2] to our case, we could estimate a systematic additional increase in the temperature difference of about 5 K between the VCSEL-aperture center and outer rim due to carrier effects.

To obtain *absolute temperatures* $T(r)$, we also take the BA-VCSEL's heat-sink temperature (set to 28 °C) into account. In addition, as the parabola emerges in the spectra only after $\sim$100 ns, we extrapolate the relative temperatures down to $\tau = 0$. This results in an offset of 5 ± 1 °C. Therefore, a constant temperature of 33 °C is added to all relative temperature shifts to obtain the absolute temperature of the cavity.

Using the spatial (radial) and temporal resolutions of the spectrally dispersed NF profiles, it is possible to determine the evolution of the absolute temperature across the radial direction of the BA-VCSEL's cavity. Figure 4 depicts five such profiles at $\tau \sim 1$ μs (full squares), 5 μs (open squares), 10 μs (full triangles), 20 μs (open circles), and 25 μs (full

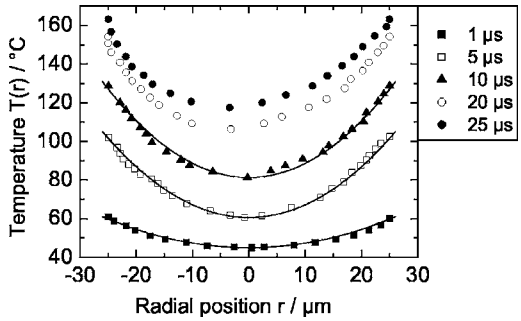

FIG. 4. Evolution of the absolute radial temperature distribution at different τ. The underlying spectral widths and radial positions were determined using the single-shot measurements recorded at different τ. Positive and negative values of r correspond to the radial direction with respect to the center of the VCSEL aperture ($r=0$), as indicated in Fig. 2. The BA-VCSEL was operated with the same conditions as in Figs. 2 and 3.

circles) for pulse amplitudes of 160 mA. The profiles include the temperature offset due to the temperature of the heat sink. The black lines in Fig. 4 represent parabolic fits ($T(r) = A + Br^2$) to guide the eye. Around 1 μs after turn-on, the temperature at the VCSEL's center is about 45 °C. The temperature increases radially with a nearly parabolic dependence. In the outer rim, the temperature amounts to about 60 °C. As can be seen in the plot, the absolute temperature increases as the pulse evolves. Moreover, the temperature difference between the outer rim and the center of the VCSEL also increases from about 15 K at $\tau \sim 1$ μs to about 50 K at $\tau \sim 10$ μs. At $\tau \sim 25$ μs the temperature in the outer region of the BA-VCSEL amounts to more than 160 °C. In addition, the profiles illustrate that the temperature distribution is increasingly asymmetric with respect to the VCSEL's center. For example, the lowest temperature at $\tau \sim 20$ μs is shifted to the left, i.e., towards negative values of r, being associated with a larger temperature gradient on the $r<0$ side of the VCSEL. This suggests that there is an asymmetry either in heat transport or in heat generation. Using such extracted temperature profiles, it is possible to study the temporal evolution of the radial temperature distribution and gain insight into the thermal processes.

In conclusion, we have introduced a scheme which allows us to determine the temporally and spatially resolved temperature profiles of BA-VCSELs. For our technique, the state of spatially incoherent emission is harnessed. The knowledge of these temperature profiles is useful for further technological development and enhancement of efficient high-power BA-VCSELs as their performance is limited by thermal effects.

The authors thank U-L-M Photonics GmbH, Ulm, Germany for providing excellent VCSEL structures.

[1] M. Grabherr, M. Miller, R. Jäger, R. Michalzik, U. Martin, H. J. Unold, and K. J. Ebeling, IEEE J. Sel. Top. Quantum Electron. **5**, 495 (1999).
[2] Y.-G. Zhao and J. G. McInerney, IEEE J. Quantum Electron. **32**, 1950 (1996).
[3] C. Degen, I. Fischer, and W. Elsäßer, Opt. Express **5**, 38 (1999).
[4] M. Brunner, K. Gulden, R. Hövel, M. Moser, and M. Ilegems, Appl. Phys. Lett. **76**, 7 (2000).
[5] C. Degen, I. Fischer, and W. Elsäßer, Appl. Phys. Lett. **76**, 3352 (2000).
[6] H. Brugger and P. W. Epperlein, Appl. Phys. Lett. **56**, 1049 (1990).
[7] M. Dabbicco, V. Spagnolo, M. Ferrara, and G. Scamarcio, IEEE J. Quantum Electron. **39**, 701 (2003).
[8] D. Lüerßen, R. J. Ram, and J. Hudgings, Proc. CLEO, CW12, 2005, Vol. 2, p. 1378.
[9] M. Peeters, G. Verschaffelt, H. Thienpont, S. K. Mandre, I. Fischer, and M. Grabherr, Opt. Express **13**, 9337 (2005).
[10] C. Degen, B. Krauskopf, G. Jennemann, I. Fischer, and W. Elsäßer, J. Opt. B: Quantum Semiclassical Opt. **2**, 517 (2000).
[11] M. Peeters, G. Verschaffelt, I. Fischer, S. K. Mandre, W. Elsäßer, J. Danckaert, and H. Thienpont, Proc. SPIE **6184**, 313 (2006).